American Mineralogist, Volume 80, pages 810–822, 1995

Armalcolite in crustal paragneiss xenoliths, central Mexico

Jodie L. Hayob,* Eric J. Essene
Department of Geological Sciences, University of Michigan, Ann Arbor, Michigan 48109, U.S.A.

Abstract

Aluminous armalcolite has been found in two sillimanite-bearing xenoliths that were recently exhumed from the lower crust of central Mexico. The ranges of compositions are $(Fe^{2+}_{0.58-0.66}Mg_{0.18-0.28}Al_{0.15-0.18}V^{3+}_{0.06-0.10}Fe^{3+}_{0.00-0.06}Ti^{4+}_{1.84-1.86})O_5$ and $(Fe^{2+}_{0.20-0.51}Mg_{0.18-0.29}Al_{0.16-0.19}V^{3+}_{0.02-0.06}Fe^{3+}_{0.30-0.81}Ti^{4+}_{1.49-1.71})O_5$. The occurrence of armalcolite is unusual in crustal paragneisses because most terrestrial armalcolite occurs in volcanic rocks that are derived from partial melting in the Earth's mantle. Textures suggest that armalcolite is a late product formed by the reaction rutile + ilmenite$_{ss}$ = armalcolite$_{ss}$ during rapid transport of the xenoliths to the surface. Phase equilibria in the system MgO-FeO-Fe_2O_3-TiO_2, which indicate that armalcolite is stable in the crust at 900–1200 °C, are consistent with this interpretation.

Thermodynamic properties are estimated for oxides in the system MgO-FeO-Fe_2O_3-TiO_2 to constrain activity-composition relations for armalcolite and conditions of formation. Activity coefficients calculated for armalcolite range from 0.27 to 1.36, depending on the ilmenite model used, at temperatures between 1000 and 1300 °C. Depth of formation of armalcolite in the crust is not well constrained. Thermodynamic calculations at 800–1200 °C for the compositions observed indicate that the armalcolite in one xenolith would have been in equilibrium with rutile at values of f_{O_2} between the hematite + magnetite buffer (HM) and the fayalite + magnetite + quartz (FMQ) buffer, and that armalcolite in the other xenolith would have been in equilibrium with rutile and ilmenite at values of f_{O_2} between FMQ and two log units below the FMQ buffer.

Introduction

Armalcolite ($Fe_{0.5}Mg_{0.5}Ti_2O_5$) has been observed most commonly in lunar rocks that equilibrated under reducing conditions, although occurrences of armalcolite in terrestrial rocks have been reported by von Knorring and Cox (1961), Ottemann and Frenzel (1965), Cameron and Cameron (1973), Haggerty (1975), Velde (1975), El Goresy and Chao (1976), Tsymbal et al. (1980), Pedersen (1981), and Mets et al. (1985). Armalcolite was discovered in two crustal xenoliths of paragneiss from central Mexico (cf. Hayob et al., 1989). The Mexican occurrence is unusual because the majority of terrestrial, armalcolite-type minerals reported thus far have been found in volcanic rocks.

Crystal chemistry of armalcolite

Armalcolite ($Mg_{0.5}Fe^{2+}_{0.5}Ti_2O_5$) forms a complete solid solution series between an Fe end-member ($Fe^{2+}Ti_2O_5$) and a Mg end-member ($MgTi_2O_5$) at high temperatures (Akimoto et al., 1957; Bowles, 1988). Armalcolite is isostructural with pseudobrookite (Psb: $Fe^{3+}_2TiO_5$), which is widespread in terrestrial volcanic rocks. Whereas Bowles's (1988) definitions of armalcolite and pseudobrookite have been accepted by the International Mineralogical Association, the definitions appear to violate the currently accepted procedure for symmetrical subdivisions of ternary composition space (Nickel, 1992). A bizarre result of Bowles's definitions is that pure $Fe^{2+}Ti_2O_5$ can be regarded as either pseudobrookite or armalcolite (Fig. 1). Nonetheless, the authors will provisionally apply the definitions of Bowles for solid solutions in the pseudobrookite group until the IMA reevaluates this system. Pseudobrookite will be used as a group name (*sensu lato*) as well as for a specific compositional range (*sensu stricto*).

Available crystal-chemical data indicate that pseudobrookite and armalcolite are entropy stabilized and therefore are expected to form at high temperatures (Navrotsky, 1975). Pseudobrookite and armalcolite have two crystallographically distinct octahedral sites, M1 (Wyckoff notation 4*c*) and M2 (Wyckoff notation 8*f*) (Smyth, 1974). Analogous to an inverse spinel structure, Fe^{3+} in ordered pseudobrookite (Fe_2TiO_5) is distributed equally between M1 and M2, and Ti^{4+} is incorporated into M2 (Lind and Housley, 1972; Brigatti et al., 1993). In ordered armalcolite, Mg^{2+} and Fe^{2+} are incorporated into M1, and Ti^{4+} is incorporated into M2 (Lind and Housley, 1972; Smyth, 1974; Wechsler et al., 1976; Brown and Navrotsky, 1989; Wechsler and von Dreele, 1989). There is, however, substantial cation disorder in most natural

* Present address: Department of Environmental Science and Geology, Mary Washington College, Fredericksburg, Virginia 22401, U.S.A.

0003–004X/95/0708–0810$02.00

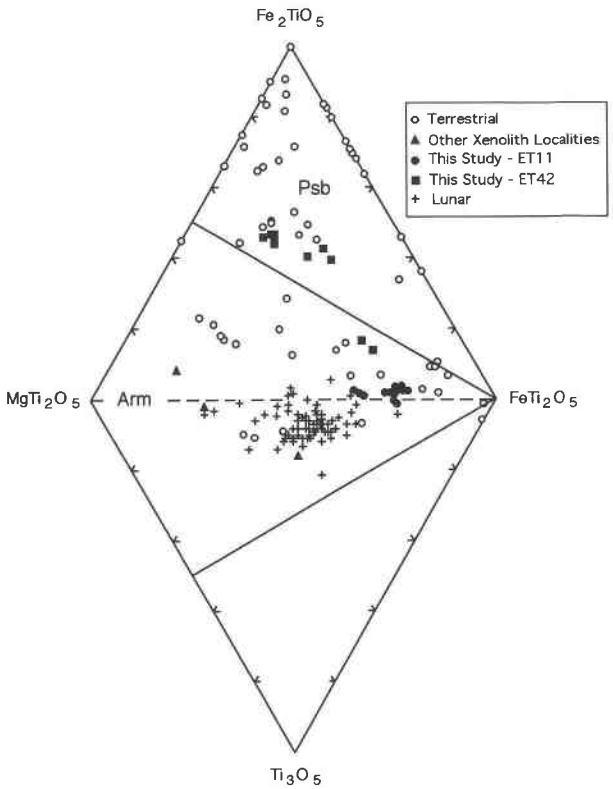

Fig. 1. Ternary composition diagrams in the systems Fe_2TiO_5-$FeTi_2O_5$-$MgTi_2O_5$ and $MgTi_2O_5$-$FeTi_2O_5$-Ti_3O_5 showing compositions of pseudobrookite and armalcolite, excluding those with >5 mol% $MnTi_2O_5$, $CaTi_2O_5$, $FeZr_2O_5$, and Cr_2TiO_5 and >10 mol% Al_2TiO_5. Terrestrial pseudobrookite: Doss (1892), Traube (1892), Palache (1935), Agrell and Langley (1958), Ottemann and Frenzel (1965), Lufkin (1976), Van Kooten (1980), Lorand and Cottin (1987), Stormer and Zhu (1994), and this study (ET42). Terrestrial armalcolite: Schaller (1912), von Knorring and Cox (1961), Ottemann and Frenzel (1965), Rice et al. (1971), Velde (1975), El Goresy and Chao (1976), Pedersen (1981), Tsymbal et al. (1982), Lorand and Cottin (1987), and this study (ET11). Other xenolith localities: Cameron and Cameron (1973) and Haggerty (1975, 1983). Lunar armalcolite: Agrell et al. (1970), Anderson et al. (1970), Haggerty et al. (1970), Kushiro and Nakamura (1970), Brett et al. (1973), Haggerty (1973a, 1973b, 1973c, 1978), El Goresy et al. (1973, 1974), Papike et al. (1974), Smyth (1974), Steele (1974), Williams and Taylor (1974), Wechsler et al. (1976), Cameron (1978), and Stanin and Taylor (1980). Arm = armalcolite, Psb = pseudobrookite.

and synthetic pseudobrookite and armalcolite (Lind and Housley, 1972; Grey and Ward, 1973; Virgo and Huggins, 1975; Wechsler, 1977; Tiedemann and Müller-Buschbaum, 1982; Wechsler and Navrotsky, 1984; Brown and Navrotsky, 1989; Wechsler and von Dreele, 1989; Brigatti et al., 1993).

Previous studies and geologic setting

Armalcolite was first identified in lunar samples from Apollo 11 (Anderson et al., 1970). Experimental data

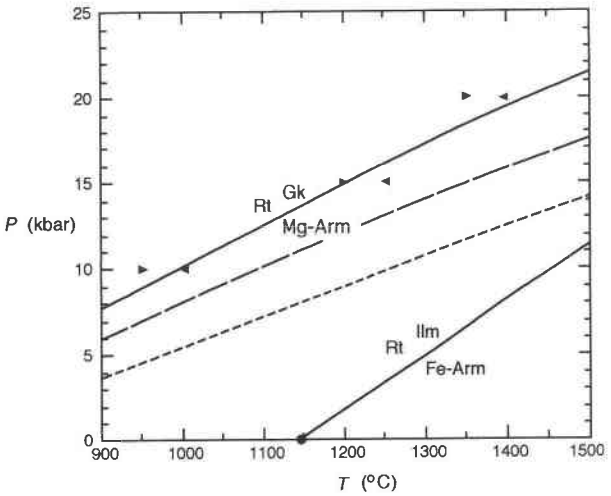

Fig. 2. *P-T* diagram showing loci of Rt + Gk = Mg-Arm and Rt + Ilm = Fe-Arm calculated from thermodynamic data in Tables 4 and 5 (solid curves). Loci of Rt + Gk = Mg-Arm calculated from thermodynamic data of Chase et al. (1985, long dashes) and Knacke et al. (1991, short dashes) are also shown. Arrows denote experimental reversals of Lindsley et al. (1974), and the solid circle is from experiments of Haggerty and Lindsley (1969). Armalcolite ($Mg_{0.5}Fe_{0.5}Ti_2O_5$) breaks down to rutile + $ilmenite_{ss}$ at 1010 °C at 1 bar (not shown; Haggerty and Lindsley, 1969). Rt = rutile, Gk = geikielite, Ilm = ilmenite, Fe-Arm = $FeTi_2O_5$, and Mg-Arm = $MgTi_2O_5$.

(Akimoto et al., 1957; Haggerty and Lindsley, 1969; Hartzman and Lindsley, 1973; Lindsley et al., 1974; Friel et al., 1977) and thermodynamic calculations (Navrotsky, 1975; Anovitz et al., 1985) indicate that $FeTi_2O_5$ is stable only at relatively low pressures and high temperatures (Fig. 2). Armalcolite occurs in lunar basalts and terrestrial volcanic rocks, consistent with an origin at low pressure and high temperature. Substitution of Al^{3+}, Cr^{3+}, and Ti^{3+} stabilizes armalcolite to lower temperature (Kesson and Lindsley, 1975), whereas addition of Zr^{4+} appears to restrict armalcolite to higher temperature (Friel et al., 1977).

Figure 1 is a diagram showing observed compositions for the system Fe_2TiO_5-$MgTi_2O_5$-$FeTi_2O_5$-Ti_3O_5 compiled for natural samples of pseudobrookite and armalcolite, excluding those with >5 mol% $MnTi_2O_5$, $CaTi_2O_5$, $FeZr_2O_5$, and Cr_2TiO_5 and >10 mol% Al_2TiO_5 (Smith, 1965; Levy et al., 1972; Peckett et al., 1972; Reid et al., 1973; Tsymbal et al., 1980; Mets et al., 1985; Varlamov et al., 1993). Experimental results of Friel et al. (1977) suggest that CaO may not be incorporated into pseudobrookite or armalcolite, and that ZrO_2 has a saturation limit in armalcolite of approximately 4 wt% at 1200–1300 °C and 1 atm, so it is uncertain whether so-called armalcolite with high CaO and ZrO_2 contents (Smith, 1965; Levy et al., 1972; Peckett et al., 1972; Reid et al., 1973) is really armalcolite. Compositions of lunar armalcolite plot near the $MgTi_2O_5$-$FeTi_2O_5$ binary or at more reducing conditions in the Ti_3O_5 field. Terrestrial

TABLE 1. Representative electron microprobe analyses of rutile associated with armalcolite

wt% oxide	ET11 Pt. 29	ET11* Pt. 30	ET42* Pt. 29	ET42 Pt. 2
ZrO_2**	1.58	1.84	1.79	1.37
SiO_2	0.02	0.01	0.00	0.00
TiO_2	96.63	96.70	95.66	96.63
Al_2O_3	0.13	0.12	0.21	0.04
Cr_2O_3	0.07	0.02	0.14	0.10
V_2O_3	0.50	0.49	0.49	0.71
Fe_2O_3	0.34	0.68	1.18	1.30
MgO	0.01	0.00	0.00	0.00
MnO	0.00	0.01	0.04	0.00
CaO	0.00	0.02	0.01	0.02
H_2O	0.12	0.15	0.25	0.25
Total	99.40	100.04	99.77	100.42
Formulae normalized to 1 cation				
Zr	0.010	0.012	0.012	0.009
Si	0.000	0.000	0.000	0.000
Ti^{4+}	0.977	0.973	0.967	0.969
Al	0.002	0.002	0.003	0.000
Cr	0.001	0.000	0.001	0.001
V	0.005	0.005	0.005	0.008
Fe^{3+}	0.003	0.007	0.012	0.013
Mg	0.000	0.000	0.000	0.000
Mn	0.000	0.000	0.000	0.000
Ca	0.000	0.000	0.000	0.000
OH†	0.011	0.014	0.021	0.022

* Inclusion in garnet.

** Similar contents of Zr have been reported in rutile associated with armalcolite by Haggerty (1987).

† OH = Al + Cr + V + Fe^{3+} (e.g., Vlassopoulos et al., 1993) assuming no substitution of Fe^{2+} or Ti^{3+}.

armalcolite typically contains a significant amount of Fe^{3+} (Fig. 1).

Several terrestrial occurrences of armalcolite and ferrous pseudobrookite are known (Fig. 1). The substance iserite, reported from Janovsky by Schaller (1912), may be armalcolite or $FeTi_2O_5$, although Janovsky considered it to be an intergrowth of rutile and Fe (wüstite or magnetite?). Von Knorring and Cox (1961) described armalcolite-pseudobrookite solid solutions in the Karroo volcanic rocks of southern Rhodesia that contain approximately equal amounts of Fe_2TiO_5, $FeTi_2O_5$, and $MgTi_2O_5$. Ottemann and Frenzel (1965) analyzed several pseudobrookite samples and an armalcolite from Germany. Rice et al. (1971) reported an analysis of armalcolite that contains approximately 80 mol% $FeTi_2O_5$ from a lamprophyre dike in New Hampshire. Armalcolite was also found by Cameron and Cameron (1973) in ultramafic nodules from Knippa Quarry, Texas, and by Haggerty (1975, 1983) from two South African kimberlite localities; armalcolite from the Dutoitspan kimberlite contains approximately 15 mol% Ti_3O_5. Armalcolite samples studied by El Goresy and Chao (1976) from the Ries impact crater in southern Germany are some of the most Fe^{2+} rich (≥80 mol% $FeTi_2O_5$ component). Terrestrial armalcolite with substantial Ti^{3+} was discovered in Mn-rich armalcolite (~20 mol% $MnTi_2O_5$) associated with native iron and graphite from the former Soviet Union (Tysmbal et al., 1980; Mets et al., 1985) and in basalts containing metallic iron and graphite from Disko Island, Greenland (Pederson, 1981). Armalcolite that is associated with native iron in trachybasalts from the Ukraine was also discovered by Tsymbal et al. (1982). Lorand and Cottin (1987) discovered armalcolite in ultrabasic cumulates from the Laouni layered intrusion in Algeria; their armalcolite analyses are similar to Velde's (1975) analyses of armalcolite from lamproites in Montana.

Armalcolite was observed in two paragneiss xenoliths (samples ET11 and ET42 of Hayob et al., 1989) from a Quaternary cinder cone, El Toro, located in the Central Mexican Plateau (CMP) near the city of San Luis Potosí. El Toro is one of several volcanic centers in the CMP that contain xenoliths from the deep crust and upper mantle (cf. Aranda-Gómez and Ortega-Gutiérrez, 1987; Hayob et al., 1989). The CMP is an elevated region of high heat flow, bounded to the west by the Sierra Madre Occidental and to the east by the Sierra Madre Oriental. The western mountains are part of an extensive, mid-Tertiary ignimbrite province, and the eastern mountains are composed of Mesozoic sediments that were deformed during the Laramide Orogeny. The younger Quaternary volcanism erupted through the CMP and alluvial cover, transporting xenoliths from the lower crust and upper mantle to the surface. More detailed field relations are given elsewhere (Aranda-Gómez, 1982; Aranda-Gómez and Ortega-Gutiérrez, 1987; Luhr et al., 1989).

PETROLOGY

The armalcolite-bearing xenoliths from El Toro contain primary garnet + sillimanite + quartz + plagioclase + mesoperthite + rutile + graphite ± ilmenite. Data for most of these minerals have been reported previously (Hayob et al., 1989) and will be discussed only briefly here. The mesoperthites consist of regular intergrowths of coarse (approximately 20 μm) alkali feldspar and plagioclase lamellae that are unusually rich in ternary feldspar components (Hayob et al., 1989, 1990). On the basis of reintegrated compositions of the mesoperthites, feldspar thermometry (Fuhrman and Lindsley, 1988) indicates that the peak of metamorphism was at $T \geq 1025$ °C (ET42) and $T \geq 1075$ °C (ET11). Compositions of coexisting host and lamellae indicate that the xenoliths last equilibrated at about 890 °C (ET42) and 880 °C (ET11) (Fuhrman and Lindsley, 1988). The garnet + sillimanite + quartz + plagioclase barometer (GASP, Koziol and Newton, 1988) yields pressures of 10.0 ± 1.0 kbar at 880 °C (ET11) and 8.9 ± 1.0 kbar at 890 °C (ET42) assuming the garnet is in equilibrium with the exsolved plagioclase.

Chemical analyses of coexisting oxides were obtained with a Cameca Camebax electron microprobe (Tables 1–3). A focused beam with an accelerating potential of 15 kV and a sample current of 0.010 μA were standard operating conditions. Well-characterized natural and synthetic materials were used as standards. Counting times of 30 s or 40000 total counts were used for all major elements in standards and unknowns. Analytical data were corrected using the Cameca PAP program. Ratios of Fe^{2+}/Fe^{3+}

TABLE 2. Representative electron microprobe analyses of ilmenite from sample ET11

wt% oxide	ET11A Rim Pt. 20	ET11B* Rim Pt. 26	ET11C Rim Pt. 8	ET11 Xtl 1 Pt. 17	ET11 Xtl 2 Pt. 5
ZrO_2	0.01	0.09	0.07	0.11	0.13
SiO_2	0.04	0.05	0.03	0.04	0.02
TiO_2	54.12	52.84	52.43	51.66	50.44
Ti_2O_3	0.10	1.95	0.00	0.00	1.83
Al_2O_3	0.05	0.15	0.17	0.10	0.24
Cr_2O_3	0.08	0.06	0.02	0.04	0.10
V_2O_3	0.50	0.38	0.46	—	0.57
Fe_2O_3	0.00	0.00	1.07	1.15	0.00
FeO	41.54	40.48	41.85	45.18	44.45
MgO	3.68	3.68	2.56	0.30	0.24
MnO	0.67	0.61	0.60	0.66	0.53
CaO	0.02	0.02	0.04	0.03	0.02
Total	100.81	100.31	99.30	99.27	98.57
Formulae normalized to 2 cations					
Zr	0.000	0.001	0.001	0.001	0.002
Si	0.001	0.001	0.001	0.001	0.000
Ti^{4+}	0.992	0.972	0.982	0.986	0.968
Ti^{3+}	0.002	0.040	0.000	0.000	0.039
Al	0.001	0.004	0.005	0.003	0.007
Cr	0.001	0.001	0.000	0.001	0.002
V	0.010	0.007	0.009	—	0.012
Fe^{3+}	0.000	0.000	0.020	0.022	0.000
Fe^{2+}	0.845	0.827	0.872	0.959	0.949
Mg	0.134	0.134	0.095	0.011	0.009
Mn	0.014	0.013	0.013	0.014	0.011
Ca	0.000	0.000	0.001	0.001	0.001
$X^{Ilm}_{MgTiO_3}$	0.134	0.134	0.095	0.011	0.009

Note: all analyses are from different crystals. Rim = rim on rutile. Xtl = discrete, homogeneous grain. $X^{Ilm}_{MgTiO_3}$ = Mg/(Mg + Fe^{2+} + Mn + 0.5Fe^{3+} + 0.5Ti^{3+} + 0.5V + 0.5Al). Fe^{3+} and Ti^{3+} were calculated from charge balance.

* Rim on rutile in garnet.

TABLE 3. Representative electron microprobe analyses of armalcolite

wt % oxide	ET11A Pt. 13	ET11B* Pt. 24	ET11C Pt. 33	ET42A Pt. 9	ET42B* Pt. 10	ET42C Pt. 19
ZrO_2	0.76	0.57	0.37	0.36	0.42	0.87
SiO_2	0.06	0.08	0.04	0.03	0.06	0.02
TiO_2	66.73	68.36	66.45	53.43	53.99	61.44
Ti_2O_3	0.71	0.00	0.00	0.00	0.00	0.00
Al_2O_3	4.21	4.12	3.72	4.38	3.79	4.11
Cr_2O_3	0.18	0.15	0.19	0.19	0.08	0.05
V_2O_3	2.47	2.00	3.23	1.25	0.75	2.09
Fe_2O_3	0.00	0.92	1.76	26.71	29.33	10.66
FeO	21.09	19.17	21.37	10.07	6.65	16.41
MgO	3.76	5.26	3.32	3.34	5.29	3.87
MnO	0.15	0.22	0.11	0.12	0.15	0.18
CaO	0.02	0.02	0.05	0.05	0.03	0.02
Total	100.14	100.87	100.61	99.93	100.54	99.72
Formulae normalized to 3 cations						
Zr	0.014	0.010	0.007	0.007	0.008	0.016
Si	0.002	0.003	0.001	0.001	0.002	0.001
Ti^{4+}	1.843	1.855	1.837	1.500	1.491	1.713
Ti^{3+}	0.021	0.000	0.000	0.000	0.000	0.000
Al	0.182	0.175	0.161	0.193	0.164	0.180
Cr	0.005	0.004	0.006	0.006	0.002	0.002
V	0.073	0.058	0.095	0.037	0.022	0.062
Fe^{3+}	0.000	0.025	0.049	0.750	0.811	0.297
Fe^{2+}	0.648	0.579	0.657	0.314	0.204	0.509
Mg	0.206	0.283	0.182	0.186	0.290	0.214
Mn	0.005	0.007	0.003	0.004	0.005	0.005
Ca	0.001	0.001	0.002	0.002	0.001	0.001
$X^{Arm}_{MgTi_2O_5}$	0.206	0.283	0.182	0.186	0.290	0.214

Note: ET11A–C are adjacent to ilmenite analyses ET11A–C in Table 2. $X^{Arm}_{MgTi_2O_5}$ = Mg/(Mg + Fe^{2+} + Mn + 0.5Fe^{3+} + 0.5V + 0.5Cr + 0.5Al + 0.5Ti^{3+}). Fe^{3+} and Ti^{3+} were calculated from charge balance.

* Inclusion in garnet.

and Ti^{3+}/Ti^{4+} were calculated by charge-balance requirements with mineral formulae normalized about cations.

In sample ET11, ilmenite occurs primarily as partial rims or overgrowths on rutile (Fig. 3a). One ilmenite crystal was observed in the matrix that is not associated with rutile or armalcolite, although it appears to be a fine intergrowth (Fig. 3b). On the basis of qualitative energy-dispersive analysis, light and dark regions are ilmenite that contains varying amounts of Fe and Mg. All Fe in ilmenite is calculated to be Fe^{2+} and most ilmenite analyses require a small amount of Ti^{3+} to maintain neutrality.

Attempts were made to determine if ilmenite in sample ET11 equilibrated with the primary mineral assemblage (e.g., garnet) by applying the K_D thermometer proposed by Powneeby et al. (1987) on the basis of the partitioning of Fe and Mn between ilmenite and garnet. However, this thermometer yields unrealistically high temperatures (>1300 °C, assuming ideal solution models), regardless of the type of ilmenite used (crystal or rim on rutile), and should not be applied to sample ET11 because the amount of Mn is very low in both ilmenite and garnet (~1 mol% in each). In addition, garnet in sample ET11 contains a substantial amount of Mg (40 mol%), the effects of which are not accounted for in the thermometer of Powneeby et al. (1987).

Although K_D thermometry suggests that some ilmenite grains may not be in equilibrium with garnet in sample ET11, barometric calculations are rather insensitive to moderate variations in the composition of ilmenite. Using ilmenite compositions ($X^{Ilm}_{FeTiO_3} \approx 0.95$), a pressure of 10.5 ± 1.0 kbar is obtained with the garnet + rutile + ilmenite + plagioclase + quartz barometer (GRIPS, Bohlen and Liotta, 1986), and 8.0 ± 1.0 kbar is obtained with the garnet + rutile + sillimanite + ilmenite + quartz barometer (GRAIL, Bohlen et al., 1983) at 880 °C. These pressures are consistent with results obtained from the GASP barometer. Textural relations suggest that ilmenite that forms rims on rutile is secondary (Fig. 3a). Pressures of 11–12 kbar (GRIPS) and 9–10 kbar (GRAIL) are obtained at 880 °C using compositions of ilmenite rims ($X^{Ilm}_{FeTiO_3} \approx 0.83$–$0.88$), indicating that the GRIPS and GRAIL barometers are quite robust with respect to moderate changes in ilmenite composition (Table 2). Ilmenite is not present in sample ET42, but limits of pressure of >8 kbar and >7 kbar, respectively, are obtained with the GRIPS and GRAIL barometers at 880 °C assuming an $a^{Ilm}_{FeTiO_3}$ of 1.0.

In sample ET11, armalcolite is associated with ilmenite that either mantles or is intergrown with rutile (Fig. 3a). Textures suggest that the armalcolite formed by decompression, as there is no evidence of injection of the basalt host near the crystals of rutile and ilmenite. Armalcolite is opaque in transmitted light and has a reflectivity similar to that of ilmenite. Minor amounts of either Fe^{3+} or

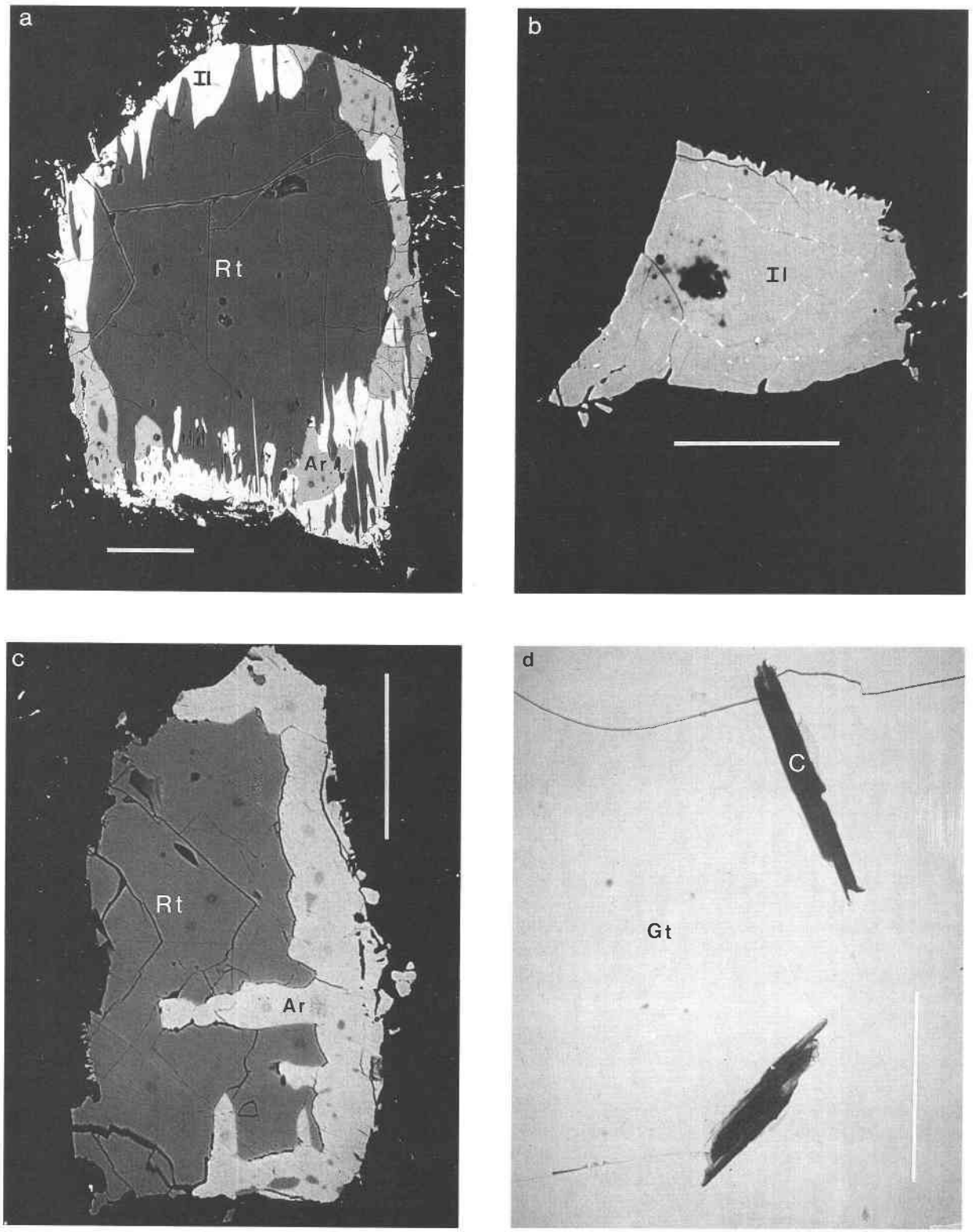

Fig. 3. Back-scattered electron (BSE) images of oxide textures. Scale bars are 50 μm. (**a**) Rutile (dark) partially rimmed by armalcolite (medium) and ilmenite (bright) from sample ET11. (**b**) Ilmenite crystal from sample ET11; light and dark regions are ilmenite that contains varying amounts of Fe and Mg. (**c**) Rutile (dark) rimmed by armalcolite (bright) from sample ET42. (**d**) Primary graphite (dark) included in garnet from sample ET11.

TABLE 4. Thermal expansion and compressibility data for phases used in this study

Phase	*a*	*b*	*c*	*d*	Ref	*e*	*f*	Ref
Rutile	-5.684×10^{-2}	2.453×10^{-3}	1.573×10^{-7}	1.247×10^{-10}	1	0.4541	0.5698	2
Geikielite	-1.123×10^{-1}	4.442×10^{-3}	1.020×10^{-6}	-1.104×10^{-10}	3	0.5917	0	4
Ilmenite	-6.830×10^{-2}	2.834×10^{-3}	8.168×10^{-8}	8.620×10^{-11}	5	0.5863	1.3006	5
$MgTi_2O_5$	-1.253×10^{-1}	5.066×10^{-3}	-5.125×10^{-6}	3.118×10^{-9}	6*	0.5917	0	7
$FeTi_2O_5$	-8.132×10^{-2}	3.458×10^{-3}	-6.064×10^{-6}	3.314×10^{-9}	3*	0.5863	1.3006	8
Fe_2TiO_5	8.381×10^{-2}	4.494×10^{-3}	-6.145×10^{-6}	3.227×10^{-9}	3*	0.5089	0.4539	9

Note: $V_T^0 = V_{298}^0 + (V_{298}^0/100)\cdot(a + bT + cT^2 + dT^3)$ (T °C); $V_T^P = V_T^0 - V_T^0(e \times 10^{-3}P - f \times 10^{-6}P^2)$ (P kbars). References are as follows: 1 = Skinner (1966); 2 = Hazen and Finger (1981); 3 = this study (see text); 4 = Liebermann (1976); 5 = Wechsler and Prewitt (1984); 6 = Brown and Navrotsky (1989); 7 = set equal to geikielite; 8 = set equal to ilmenite; 9 = set equal to hematite (Robinson et al., 1982).

* Valid only for T = 700–1200 °C.

Ti^{3+} are required in armalcolite analyses to satisfy charge balance, whereas ilmenite analyses require a small amount of Ti^{3+}. The apparent need for trivalent ions in ilmenite may be the result of small systematic errors in the microprobe data, particularly since Ti^{3+} is preferentially partitioned into armalcolite rather than ilmenite (Lindsley et al., 1974; Kesson and Lindsley, 1975). In sample ET42, armalcolite is associated only with rutile (Fig. 3c). In this sample, there is also no evidence of injection of the basalt host near the crystals of rutile and armalcolite, although both are associated with quenched isochemical melt that rims garnets. It is possible that the armalcolite formed by the reaction of rutile with Fe from the nearby garnet or from ilmenite that is no longer present. Variable but substantial amounts of Fe^{3+} are needed in this armalcolite to maintain neutrality (Table 3). The $X^{Ilm}_{MgTiO_3}$ in sample ET11 ranges from 0.09 to 0.13 and the $X^{Arm}_{MgTi_2O_5}$ ranges from 0.18 to 0.28 (Tables 2 and 3), corresponding to a range in K_D of 2.2–2.6 [$K_D = (Mg/Fe^{2+})^{Arm}(Mg/Fe^{2+})^{Ilm}$]. In contrast, experimental results of Lindsley et al. (1974) at 1 bar suggest that the distribution coefficient between armalcolite and ilmenite has a value between 3.6 and 4.8 for temperatures of 900–1140 °C. Their data predict the ilmenite with 9–13 mol% $MgTiO_3$ should be in equilibrium with armalcolite that contains 30–40 mol% $MgTi_2O_5$. The discrepancy in K_D predicted from the experiments and that observed for the Mexican samples may result from errors in the experiments, disequilibrium in the natural samples, or both. Upper limits of pressure can nonetheless be estimated for the formation of armalcolite from ln K calculated as a function of pressure for the breakdown of rutile + geikielite to $MgTi_2O_5$ from the reaction

$$TiO_2 + MgTiO_3 = MgTi_2O_5 \qquad (1)$$

which has been located for the range T = 950–1400 °C by Lindsley et al. (1974) (Fig. 2). If the rutile, ilmenite, and armalcolite were in equilibrium, pressures can be estimated from values of ln K for Equilibrium 1. Use of Equilibrium 1 for barometry of natural samples, however, requires knowledge of the thermodynamic properties of pure $MgTi_2O_5$ and activity relations for armalcolite solid solutions.

THERMODYNAMIC PROPERTIES OF OXIDES IN THE SYSTEM MgO-FeO-Fe_2O_3-TiO_2

Data are not available for the thermal expansion of $MgTiO_3$ or for the compressibility of $MgTi_2O_5$. Therefore, the coefficients of thermal expansion (*a, b, c,* and *d*) for geikielite were estimated from the equation in Table 4 and

$$V(MgTiO_3) = V(FeTiO_3) + V(MgO) - V(FeO). \qquad (2)$$

Thermal expansivities of FeO (stoichiometric) and MgO were obtained from Fei and Saxena (1986). Thermal expansion coefficients for $MgTi_2O_5$ were derived from high-temperature in situ diffraction data of Brown and Navrotsky (1989) for the temperature range 700–1200 °C and may not be valid outside of this range. The compressibility of $MgTi_2O_5$ was set equal to that of $MgTiO_3$ because compressibility data are not available.

High-temperature, in situ X-ray powder diffraction data of Brown and Navrotsky (1989) indicate that disorder in $MgTi_2O_5$ increases continuously from 500 to 1200 °C (and probably up to 1500 °C). Disorder in $MgTi_2O_5$ above about 1000 °C, however, is not preserved in quenched samples (Wechsler and Navrotsky, 1984; Brown and Navrotsky, 1989; Wechsler and von Dreele, 1989). Entropy coefficients of $MgTi_2O_5$ are derived from high-temperature heat content data of $MgTi_2O_5$ (Brown and Navrotsky, 1989) using transposed temperature-drop calorimetry (Table 5). Thus, the entropy coefficients for $MgTi_2O_5$ derived from those enthalpy data should include any contributions to entropy that result from disorder. The S^0_{298} of $MgTi_2O_5$ is from Kelley and King (1961) with an additional 10.5 J/(mol·K) added for the third law entropy at 0 K (Table 5), which was estimated from cation distribution data on samples quenched from 973 K (Brown and Navrotsky, 1989). However, these entropy coefficients are valid only for the temperature range of the enthalpy measurements (700–1500 °C) and should not be used outside of this range. Thus, standard free energies of formation cannot be estimated at 298.15 K for pseudobrookite from the data in Tables 4 and 5. In contrast, thermochemical data and room-temperature Rietveld re-

TABLE 5. Molar volume, entropy, and entropy coefficients for phases used in this study

Phase	V^0_{298} (cm³/mol)	Ref	S^0_{298} [J(mol·K)]	Ref	A	B	C	D	Ref
Rutile	18.82	1	50.29	1	62.852	11.363	4.991	−367.10	1
Geikielite	30.86	1	74.56	2	118.365	13.723	13.661	−693.79	3
Ilmenite	31.70	4	108.91	4	125.222	13.184	14.886	−734.04	4
$MgTi_2O_5$	54.87	5	137.65	6	205.200	20.736	49.827	−1231.31	7*
$FeTi_2O_5$	55.75	5	172.21	6	212.057	20.200	51.053	−1271.60	6*
Fe_2TiO_5	54.53	1	172.38	6	192.589	22.008	15.502	−1121.27	8

Note: $S^0_T - S^0_{298} = A \ln T + B \times 10^{-3} T + C \times 10^5 T^{-2} + D(T\,\mathrm{K})$. References are as follows: 1 = Robie et al. (1978); 2 = Kelley and King (1961); 3 = Naylor and Cook (1946); 4 = Anovitz et al. (1985); 5 = Lindsley et al. (1974); 6 = this study (see text); 7 = Brown and Navrotsky (1989); 8 = Bonnickson (1954).

* Valid only for T = 700–1500 °C.

finements of the structure of geikielite quenched from high temperature suggest that Mg and Ti are completely ordered in the two octahedral sites up to temperatures of at least 1400 °C (Wechsler and von Dreele, 1989). Entropy data for geikielite in Table 5 were taken directly from measured values (Naylor and Cook, 1946; Kelley and King, 1961) without correction for zero-point entropy.

The location of Equilibrium 1 was calculated from available thermodynamic data with the assumption that ΔG_r (1) equals 0 at 1200 °C and 15 kbar (Fig. 2), on the basis of the experimental reversal of Lindsley et al. (1974). Data used in all thermodynamic calculations are given in Tables 4 and 5. The calculated locus of Equilibrium 1 fits the experimental brackets between 950 and 1200 °C but is located at temperatures that are too high by at least 25 °C at 20 kbar (Fig. 2). Although the equilibrium is not tightly reversed, results of the experiments suggest a somewhat flatter slope between 900 and 1200 °C and greater slope between 1200 and 1400 °C (using midpoints of reversals). Curves calculated from Gibbs free energy data tabulated in Chase et al. (1985) and Knacke et al. (1991) with thermal expansivities and compressibilities from Table 4 are located at pressures that are too low by an average of 3 and 5 kbar, respectively, for a given temperature, and their slopes are somewhat flatter than the calculated curve (Fig. 2). Evans and Muan (1971) calculated the free energies of formation of $MgTiO_3$ and $MgTi_2O_5$ from the oxides at 1 bar and 1400 °C on the basis of CO-CO_2 ratios in equilibrium with Ni and Mg titanates. They obtained a value of ΔG_r for Equilibrium 1 of −9.2 kJ/mol at 1 bar and 1400 °C (cf. Navrotsky, 1975), in good agreement with a value of −9.6 kJ/mol calculated in this study. Chase et al. (1985) reported a value for ΔG_r of Equilibrium 1 of −7.9 kJ/mol, whereas Knacke et al. (1991) obtained −6.3 kJ/mol at 1 bar and 1400 °C. These data are inconsistent with experiments on Reaction 1 and are disregarded in this study (Fig. 2).

Experimental data at pressures greater than 1 bar are not available for the reaction

$$TiO_2 + FeTiO_3 = FeTi_2O_5 \quad (3)$$

located at 1140 °C and 1 bar (Haggerty and Lindsley, 1969). Because molar volume data are available only at STP for $FeTi_2O_5$, thermal expansion and compressibility of $FeTi_2O_5$ were estimated from values and equations in Table 4 and

$$V(FeTi_2O_5) = V(MgTi_2O_5) + V(FeO) - V(MgO). \quad (4)$$

Thermal expansion and compressibility data for FeO (stoichiometric) and MgO (Fei and Saxena, 1986) were refit to the equations given in Table 4.

Anovitz et al. (1985) estimated the entropy of $FeTi_2O_5$ from those of pseudobrookite, hematite, and ilmenite. They assumed that Fe_2TiO_5 and $FeTi_2O_5$ were completely ordered (normal pseudobrookite structure of $TiFe_2O_5$) and did not account for entropy from magnetic effects. Their analysis yields a value of S^0_{298} = 156.1 J/(mol·K). Because most crystals of pseudobrookite contain a substantial amount of disorder at T > 700 °C (Brown and Navrotsky, 1989; Brigatti et al., 1993), a better approximation of S^0_{298} and entropy coefficients (A, B, C, and D) of $FeTi_2O_5$ can be estimated from

$$S^0(FeTi_2O_5) = S^0(MgTi_2O_5) + S^0(FeTiO_3) - S^0(MgTiO_3) + 2.5V^0 \quad (5)$$

(Fyfe and Verhoogen, 1958) and

$$V(FeTi_2O_5) = V(MgTi_2O_5) + V(FeTiO_3) - V(MgTiO_3) \quad (6)$$

(Table 5). An estimate of S^0_{298} = 172.4 J/(mol·K) is obtained for $FeTi_2O_5$, significantly higher than the value estimated by Anovitz et al. (1985). Inherent in Equation 5 is the assumption that $FeTi_2O_5$ and $MgTi_2O_5$ exhibit similar degrees of disorder with increasing temperature. There are no in situ cation distribution data available for $FeTi_2O_5$, but a comparison of cation distribution data for synthetic, quenched samples of $FeTi_2O_5$ and $MgTi_2O_5$ suggests that $FeTi_2O_5$ has similar amounts of cation ordering (Lind and Housley, 1972; Grey and Ward, 1973; Virgo and Huggins, 1975; Brown and Navrotsky, 1989; Wechsler and von Dreele, 1989). Ilmenite (Ishikawa and Akimoto, 1957; Stickler et al., 1967) and pseudobrookite (Akimoto et al., 1957; Muranaka et al., 1971) are paramagnetic at room temperature and become antiferromagnetic at low temperature. As a first approximation, con-

tributions to the configurational entropy of $FeTi_2O_5$ resulting from magnetic transitions at low temperature are accounted for in Relation 5 because magnetic effects are included in the entropy data of ilmenite (Anovitz et al., 1985). Heat capacity, transposed drop calorimetry, and in situ cation distribution data at high temperature are necessary for a more accurate determination of the thermodynamic properties of $FeTi_2O_5$.

Thermodynamic data used for pseudobrookite are given in Tables 4 and 5. The thermal expansion of Fe_2TiO_5 was estimated from

$$V(Fe_2TiO_5) = V(FeTi_2O_5) + V(Fe_2O_3) - V(FeTiO_3) \quad (7)$$

(Table 4). The compressibility of pseudobrookite was set equal to that of hematite. Thermodynamic data of Robinson et al. (1982) were used for hematite. The S^0_{298} of pseudobrookite was estimated from

$$S^0(Fe_2TiO_5) = S^0(FeTi_2O_5) + S^0(Fe_2O_3) - S^0(FeTiO_3) + 2.5V^0 \quad (8)$$

(Fyfe and Verhoogen, 1958). Using entropy coefficients estimated from $FeTi_2O_5$, Fe_2O_3, and $FeTiO_3$, values of $S^0_T - S^0_{298}$ calculated for pseudobrookite are slightly lower than published values of $S^0_T - S^0_{298}$. Therefore, entropy coefficients for pseudobrookite were taken directly from the published values of Bonnickson (1954).

Activity-composition relations of armalcolite

Activity-composition (a-X) relations have been evaluated for ilmenite-geikielite-hematite solid solutions (Andersen and Lindsley, 1988; Ghiorso, 1990; Andersen et al., 1991), although some discrepancies remain in these values that may be traced to the mixing properties assumed for olivine. No mixing data are available for orthorhombic oxides in the ternary system $FeTi_2O_5$-$MgTi_2O_5$-Fe_2TiO_5. The Fe-Mg exchange equilibrium between stoichiometric armalcolite (i.e., $Fe_{0.5}Mg_{0.5}Ti_2O_5$) and ilmenite$_{ss}$

$$MgTiO_3 + FeTi_2O_5 = FeTiO_3 + MgTi_2O_5 \quad (9)$$

was located at 1010 °C at 1 bar by Lindsley et al. (1974). The composition of ilmenite in equilibrium with $Fe_{0.5}Mg_{0.5}Ti_2O_5$ is $Fe_{0.8}Mg_{0.2}TiO_3$ (their Fig. 1), although exact compositions or chemical analyses are not given. They studied the equilibrium distribution of Fe^{2+} and Mg between armalcolite and ilmenite for a range of bulk compositions at 1 bar and 900–1140 °C. A value of K_D between 3.6 and 4.8 is calculated from their data. Friel et al. (1977) determined the location of Equilibrium 9 for stoichiometric armalcolite for the temperature range 1000–1200 °C as a function of pressure, although they did not report the composition of ilmenite in equilibrium with $Fe_{0.5}Mg_{0.5}Ti_2O_5$. On the basis of the K_D data of Lindsley et al. (1974), $Fe_{0.5}Mg_{0.5}Ti_2O_5$ should have equilibrated with $Fe_{0.825}Mg_{0.175}TiO_3$ at 1100 °C and with $Fe_{0.85}Mg_{0.15}TiO_3$ at 1200 °C, if the K_D is independent of pressure.

Mixing relations can be estimated for $FeTi_2O_5$-$MgTi_2O_5$ solutions using experimental results for Equilibria 1, 3, and 9 if the following are accurately known: (1) volume data of all phases at P and T, (2) a-X relations of ilmenite-geikielite solutions, and (3) $K_D = (Mg/Fe)^{Arm}/(Mg/Fe)^{Ilm}$ as a function of P and T. Volume data used in this study are given in Tables 4 and 5. Mixing relations of Andersen et al. (1991) and Ghiorso (1990) were used for ilmenite-geikielite solid solutions, and an ideal model was assumed for rutile. The K_D was estimated as a function of temperature from the data of Lindsley et al. (1974). Activity coefficients for $FeTi_2O_5$ and $MgTi_2O_5$ calculated from

$$\int_{P'}^{P} \Delta V_R \, dP = -RT \ln \frac{K}{K'} \quad (10)$$

are given in Table 6. The prime refers to the standard state, chosen to be either $MgTi_2O_5$ or $FeTi_2O_5$ for armalcolite at T of interest, where P' is defined by the locus of Equilibrium 1 or 3, respectively. Assuming a molecular activity model (i.e., $a^{Arm}_{MgTi_2O_5} = \gamma^{Arm}_{MgTi_2O_5} \cdot X^{Arm}_{MgTi_2O_5}$), negative deviations from ideality are necessary for $MgTi_2O_5$, and positive deviations are required for $FeTi_2O_5$ for the shifted loci of Equilibria 1 and 3 to be coincident with the locus of Equilibrium 9 (Table 6). Regardless of the ilmenite model used, the calculated activity coefficients of $MgTi_2O_5$ and $FeTi_2O_5$ decrease with increasing temperature.

Table 6. Calculated activity coefficients for armalcolite ($Fe_{0.5}Mg_{0.5}Ti_2O_5$) on the basis of a molecular activity model

T (°C)	ABL $\gamma^{Arm}_{MgTi_2O_5}$	G $\gamma^{Arm}_{MgTi_2O_5}$	ABL $\gamma^{Arm}_{FeTi_2O_5}$	G $\gamma^{Arm}_{FeTi_2O_5}$
1010	0.78	1.02	n.d.	n.d.
1100	0.56	0.81	n.d.	n.d.
1140	n.d.	n.d.	1.30	1.36
1200	0.42	0.67	1.28	1.33
1300	0.27	0.50	1.21	1.24

Note: ABL values calculated using a-X relations of ilmenite from Andersen et al. (1991); G values calculated using a-X relations of ilmenite from Ghiorso (1990); n.d. = not determined.

Barometry

Pressures were estimated from Relation 10 with P' defined by the locus of Equilibrium 1 or Equilibrium 3 for rutile-armalcolite ± ilmenite pairs from samples ET11 and ET42, assuming various activity models for armalcolite and ilmenite (Hayob, 1994). Attempts to use the derived thermodynamic values to estimate pressure of formation of armalcolite were not successful. It is likely that the ilmenite and armalcolite did not equilibrate in sample ET11, on the basis of low values obtained for the K_D in comparison with data of Lindsley et al. (1974). Upper limits of pressure estimated from armalcolite compositions are not useful because of the substantial dilution of the $MgTi_2O_5$ and $FeTi_2O_5$ components, and it is difficult to evaluate the effect of additional components such as Al on the stability of armalcolite in the xenoliths. The depth in the crust at which armalcolite formed in the xenoliths cannot be well constrained. However, by anal-

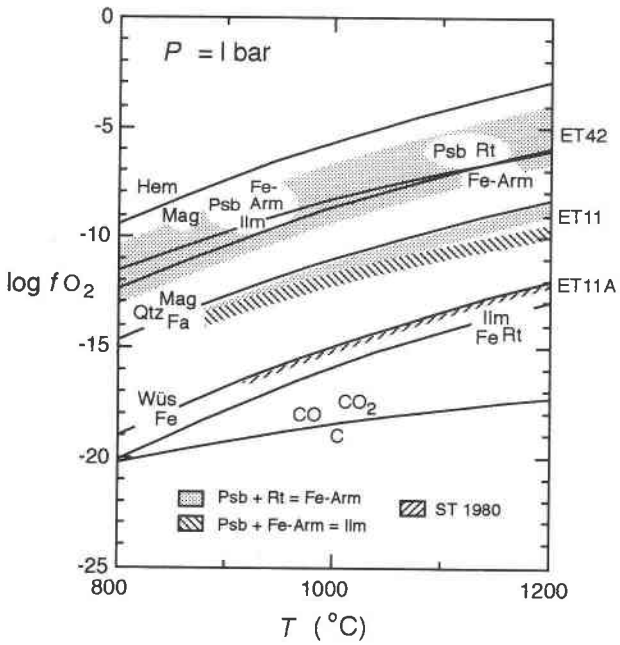

Fig. 4. Log f_{O_2}-T diagram at 1 bar total pressure and 800–1200 °C showing loci of Equilibria 11 and 12 (combined), 16, and 17. Equilibria 16 and 17 are metastable below 1140 °C, where $FeTi_2O_5$ breaks down to rutile + ilmenite. Lined field shows ranges in f_{O_2} calculated from Equilibrium 16 for sample ET11. Light stippled field represents ranges in f_{O_2} calculated from Equilibrium 17 for samples ET11 and ET42, and heavy stippled line is calculated from the Ti^{3+} content of armalcolite for sample ET11A (Stanin and Taylor, 1980: ST). The reactions hematite = magnetite + O_2, quartz + magnetite = fayalite + O_2, and wüstite = iron + O_2 were calculated from equilibrium expressions in Frost (1991); ilmenite = rutile + iron + O_2 was calculated from thermodynamic data referenced in this study. C = graphite, CO = carbon monoxide, CO_2 = carbon dioxide, Fa = fayalite, Fe = metallic iron, Fe-Arm = $FeTi_2O_5$, Hem = hematite, Ilm = ilmenite, Mag = magnetite, Psb = pseudobrookite, Qtz = quartz, Rt = rutile, Wus = wüstite.

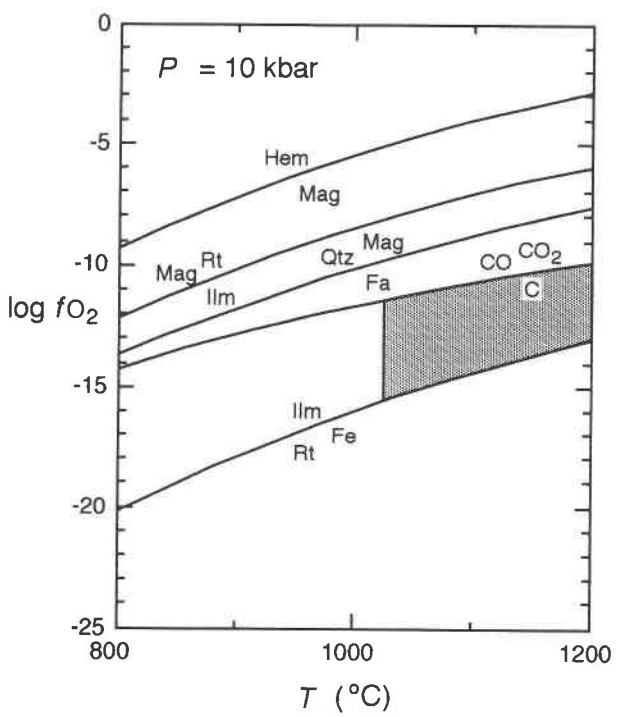

Fig. 5. Log f_{O_2}-T diagram at 10 kbar total pressure and 800–1200 °C. Stippled field shows range in f_{O_2} conditions for the peak of metamorphism. Magnetite + rutile = ilmenite was calculated from thermodynamic data referenced in this study and data for magnetite from Robie et al. (1978). Hematite = magnetite, quartz + magnetite = fayalite, ilmenite = rutile + Fe, and abbreviations as in Fig. 4.

ogy with other armalcolite occurrences and from textural criteria, it seems likely that the Mexican armalcolite formed during decompression.

Implications for redox conditions

Metamorphic peak f_{O_2}

Primary graphite, occurring as flakes along grain boundaries and as inclusions in other primary minerals, is common in both xenoliths (e.g., Fig. 3d). In the presence of graphite (a_C = 1), the partial pressure (and fugacity) of O_2 in equilibrium with graphite is buffered by the equilibria

$$C + \tfrac{1}{2}O_2 = CO \quad (11)$$

$$C + O_2 = CO_2 \quad (12)$$

and

$$P_{CO} + P_{CO_2} = P_{tot} \quad (13)$$

assuming that $P_{fluid} = P_{tot}$ and P_{H_2O} has negligible contributions to total pressure. At 1 bar total pressure, the partial pressure of each gaseous species can be determined as a function of temperature from

$$\Delta G^0_T = -RT \ln K. \quad (14)$$

Gibbs free energy data from Robie et al. (1978) were used to calculate the location of Equilibria 11 and 12 for the range T = 800–1200 °C at 1 bar total pressure (Fig. 4), assuming an ideal model ($P_i = f_i$). Oxygen fugacities more reducing than those of the iron + wüstite (IW) buffer are necessary to stabilize graphite at high temperatures at 1 bar (Fig. 4).

Pressure has a large effect on the locations of Equilibria 11 and 12 in f_{O_2}-T space (e.g., Nordstrom and Munoz, 1986). At $P_{tot} > 1$ bar,

$$\Delta G^P_T \approx -RT \ln K + \Delta V^0_{298}\,(\text{solids})\,\Delta P. \quad (15)$$

An iterative method was used to calculate the f_{O_2} of Equilibria 11 and 12 using Assumption 13 and Expression 15 at 10 kbar total pressure (Fig. 5). Fugacities were calculated from fugacity coefficients for CO (Ryzhenko and Volkov, 1971) and CO_2 (Shmulovich and Shmonov, 1975) at P and T up to 10 kbar and 1200 °C. The calculations were reiterated until convergence was achieved between

the initial and final values for the partial pressures of CO and CO_2. The calculated f_{O_2} for Equilibria 11 and 12 is not extremely sensitive to the values of fugacity coefficients for CO and CO_2 or to the ratio of CO/CO_2. For example, at 900 °C γCO_2 = 11.31–15.02 if P_{CO_2} = 8–9 kbar (Shmulovich and Shmonov, 1975), and γCO = 1.87–1.37 if P_{CO} = 1–2 kbar (Ryzhenko and Volkov, 1971), resulting in a calculated range in $-\log f_{O_2}$ of 12.87–12.79. Convergence is obtained at 900 °C and 10 kbar total pressure for values of P_{CO} = 1.57 kbar and P_{CO_2} = 8.43 kbar, corresponding to $-\log f_{O_2}$ = 12.83. Figures 4 and 5 show the calculated locations of Equilibria 11 and 12 (combined) at 1 bar and 10 kbar, respectively, at 800–1200 °C. If other fluid species were present, the activities of CO and CO_2 would be reduced and the loci of the combined equilibria (from 11 and 12) would be shifted toward lower values of $-\log f_{O_2}$ in Figures 4 and 5. Thus, the presence of graphite provides an upper limit for the f_{O_2} at which the xenoliths equilibrated at approximately 10 kbar total pressure (Fig. 5).

The presence of primary graphite, lack of metallic Fe, and pressure estimates of 10 kbar for the peak of metamorphism indicate that the xenoliths equilibrated at values of $-\log f_{O_2}$ between 11 and 15 during the peak of metamorphism at 1025–1075 °C (Fig. 5), the minimum temperature for the peak of metamorphism estimated on the basis of feldspar thermometry in these samples (Hayob et al., 1989).

Armalcolite formation f_{O_2}

Phase equilibria involving armalcolite can be used to constrain f_{O_2} conditions if the armalcolite + rutile ± ilmenite were in equilibrium. In an oxidizing atmosphere at high temperature and low total pressure, ilmenite forms an armalcolite-pseudobrookite solid solution

$$3FeTiO_3 + \tfrac{1}{2}O_2 = Fe_2TiO_5 + FeTi_2O_5 \qquad (16)$$

and $FeTi_2O_5$ oxidizes to form rutile + pseudobrookite

$$2FeTi_2O_5 + \tfrac{1}{2}O_2 = 3TiO_2 + Fe_2TiO_5 \qquad (17)$$

(Anovitz et al., 1985). These O_2 buffers are located within one log unit of each other at 1 bar total pressure between the hematite + magnetite (HM) and FMQ buffers (Fig. 4). Equilibria 16 and 17 are metastable below 1140 °C at 1 bar because $FeTi_2O_5$ is not stable.

It is difficult to estimate the temperature of formation of armalcolite in the xenoliths. The high Fe^{2+} content of armalcolite in sample ET11 suggests that armalcolite formed at fairly high temperature; however, Ti^{3+} and Al should stabilize armalcolite to lower temperatures (Kesson and Lindsley, 1975). The effect of V^{3+} on the stability of armalcolite has not been studied experimentally but (by analogy with other trivalent ions) V should stabilize armalcolite. Two-feldspar thermometry of the exsolved feldspars indicates that the xenoliths did not cool below 900 °C until after eruption (Hayob et al., 1989, 1990). Data from Beard et al. (1993), which compare the feldspar thermometer of Elkins and Grove (1990) with experimental results on Kilbourne Hole xenoliths, suggest that feldspar thermometry has an accuracy of better than ±50 °C. The thermometer of Elkins and Grove (1990) yields temperatures that are similar to the models of Fuhrman and Lindsley (1988) and Lindsley and Nekvasil (1989) that were used by Hayob et al. (1989). Melting experiments conducted by Beard et al. (1993) on a pelite (their sample KH-12) from Kilbourne Hole at 900–1000 °C produced no melt, indicating that pelites may be quite refractory and stable to temperatures >1000 °C. There is no textural evidence of reheating of the xenoliths during decompression. Rims of quenched melt that formed upon decompression (Hayob et al., 1989) surround garnet in both samples and a small amount of melt (<1% by volume) is present along some grain boundaries. However, zoning is absent in all minerals, and if reheating occurred, it happened rapidly enough such that the compositions of the primary minerals were not affected. Thus, it is reasonable to assume that armalcolite formed at about 900–1000 °C at pressures lower than the peak of metamorphism (10 kbar).

Incorporation of activity coefficients has a negligible effect (e.g., ±0.1 log unit) on the calculated values of log f_{O_2} (±0.1 log unit) for ET11 and ET42 in comparison with the effect of chemical heterogeneity in the oxides. Therefore, ideal molecular activity models were used for all phases (i.e., $a^{Psb}_{Fe_2TiO_5} = X^{Psb}_{Fe_2TiO_5}$). Values of log f_{O_2} estimated at 1 bar from Equilibrium 16 for sample ET11, which contains ilmenite, and Equilibrium 17 for ET11 and ET42 are shown in Figure 4. At 10 kbar, Equilibria 16 and 17 are shifted +1.2 and 0.0 log units, respectively, from the 1 bar loci. The range of log f_{O_2} indicated for each sample represents variations in log f_{O_2} resulting from chemical heterogeneity in the coexisting oxides (Tables 1–3). In sample ET42, the mole fraction of $FeTi_2O_5$ is diluted sufficiently that armalcolite is stable to temperatures <800 °C (e.g., Fig. 2). Armalcolite from sample ET11, however, is not stable below 900 °C (Fig. 4) on the basis of values of log K for Equilibrium 3. Equilibria 16 and 17 cannot be applied to armalcolite ET11A, which lacks a pseudobrookite component and contains a small amount of Ti^{3+}. Stanin and Taylor (1980) formulated an O_2 barometer for lunar basalts on the basis of the amount of Ti^{3+} in armalcolite and proposed that Ti^{3+}-rich armalcolite typically equilibrates at values of log f_{O_2} between IW and 1.5 log units below IW. Their results are consistent with experiments of Friel et al. (1977) in which armalcolite reacted to form ilmenite + reduced armalcolite at values of log f_{O_2} below −10.5 at 1200 °C and 1 bar. From the expression

$$\log f_{O_2} = -1.7\left(\frac{X_{Ti^{3+}}}{X_{Fe^{2+}}}\right) \qquad (18)$$

(Stanin and Taylor, 1980), a value for log f_{O_2} of approximately 0.0 (Fig. 4) is obtained for armalcolite from ET11A (heavy shaded curve, Fig. 4), where the f_{O_2} is in log units relative to the iron + wüstite buffer. In Equation

18, Ti^{3+} is the mole fraction of Ti_3O_5 and Fe^{2+} is the mole fraction of $FeTi_2O_5$ in armalcolite.

Discussion

Chemical variation in armalcolite produces a large range in calculated f_{O_2} for both samples, which may indicate disequilibrium on the scale of a thin section. The range in f_{O_2} is typical, however, for crustal and mantle rocks and indicates that armalcolite solid solutions involving Fe^{2+} and Mg are stable in terrestrial rocks. The value of f_{O_2} near IW for sample ET11A is more typical of lunar rocks, but the calculated f_{O_2} is sensitive to small amounts of Ti^{3+}. Armalcolite seems to be relatively rare, however, even in volcanic rocks, and bulk composition may be more important than P-T-f_{O_2} in controlling its stability (Anovitz et al., 1985).

Acknowledgments

This research was supported by National Science Foundation grants EAR-89017772 and EAR-91017772 to E.J.E., the Sigma Xi Research Society, and the Scott Turner Fund of the University of Michigan. The authors thank E. Zbinden and S. Haggerty for their reviews, which improved the clarity of the manuscript. Helpful discussions were provided by S. Bohlen, J. O'Neil, and D. Peacor. J. Ruiz, F. Ortega-Gutiérrez, and J. Aranda-Gómez are thanked for their assistance in the field. This work is contribution no. 501 from the Mineralogical Laboratory, University of Michigan.

References cited

Agrell, S.O., and Langley, J.M. (1958) The dolerite plug at Tievebulliagh near Cushendall, Co. Antrim. Proceedings of the Royal Irish Academy, Section B, 59, 63–127.

Agrell, S.O., Scoon, J.H., Muir, I.D., Long, J.V.P., McConnell, J.D.C., and Peckett, A. (1970) Observations on the chemistry, mineralogy and petrology of some Apollo 11 lunar samples. Proceedings of the Apollo 11 Lunar Science Conference. Geochimica et Cosmochimica Acta, Supplement 1, 1, 93–128.

Akimoto, S., Nagata, T., and Katsura, T. (1957) The $TiFe_2O_5$-Ti_2FeO_5 solid solution series. Nature, 179, 37–38.

Andersen, D.J., and Lindsley, D.H. (1988) Internally consistent solution models for Fe-Mg-Mn-Ti oxides: Fe-Ti oxides. American Mineralogist, 73, 714–726.

Andersen, D.J., Bishop, F.C., and Lindsley, D.H. (1991) Internally consistent solution models for Fe-Mg-Mn-Ti oxides: Fe-Mg-Ti oxides and olivine. American Mineralogist, 76, 427–444.

Anderson, A.T., Bunch, T.E., Cameron, E.N., Haggerty, S.E., Boyd, F.R., Finger, L.W., James, O.B., Keil, K., Prinz, M., Ramdohr, P., and El Goresy, A. (1970) Armalcolite: A new mineral from the Apollo 11 samples. In A.A. Levinson, Ed., Proceedings of the Apollo 11 lunar science conference, p. 55–63. Pergamon, New York.

Anovitz, L.M., Treiman, A.H., Essene, E.J., Hemingway, B.S., Westrum, E.F., Jr., Wall, V.J., Burriel, R., and Bohlen, S.R. (1985) The heat capacity of ilmenite and phase equilibria in the system Fe-Ti-O. Geochimica et Cosmochimica Acta, 49, 2027–2040.

Aranda-Gómez, J.J. (1982) Ultramafic and high grade metamorphic xenoliths from central Mexico, 236 p. Ph.D. thesis, University of Oregon, Eugene, Oregon.

Aranda-Gómez, J.J., and Ortega-Gutiérrez, F. (1987) Mantle xenoliths in Mexico. In P.H. Nixon, Ed., Mantle xenoliths, p. 75–84. Wiley, New York.

Beard, J.S., Abitz, R.J., and Lofgren, G.E. (1993) Experimental melting of crustal xenoliths from Kilbourne Hole, New Mexico, and implications for the contamination and genesis of magmas. Contributions to Mineralogy and Petrology, 115, 88–102.

Bohlen, S.R., and Liotta, J.J. (1986) A barometer for garnet amphibolites and garnet granulites. Journal of Petrology, 27, 1025–1034.

Bohlen, S.R., Wall, V.J., and Boettcher, A.L. (1983) Experimental investigations and geological applications of equilibria in the system FeO-TiO_2-Al_2O_3-SiO_2-H_2O. American Mineralogist, 68, 1049–1058.

Bonnickson, K.R. (1954) High temperature heat contents of some titanates of aluminum, iron and zinc. Journal of the American Chemical Society, 77, 2152–2154.

Bowles, J.F.W. (1988) Definition and range of composition of naturally occurring minerals with the pseudobrookite structure. American Mineralogist, 73, 1377–1383.

Brett, R., Gooley, R.C., Dowty, E., Prinz, M., and Keil, K. (1973) Oxide minerals in lithic fragments from Luna 20 fines. Geochimica et Cosmochimica Acta, 37, 761–773.

Brigatti, M.F., Contini, S., Capedri, S., and Poppi, L. (1993) Crystal chemistry and cation ordering in pseudobrookite and armalcolite from Spanish lamproites. European Journal of Mineralogy, 5, 73–84.

Brown, N.E., and Navrotsky, A. (1989) Structural, thermodynamic, and kinetic aspects of disordering in the pseudobrookite-type compound karrooite, $MgTi_2O_5$. American Mineralogist, 74, 902–912.

Cameron, E.N. (1978) An unusual titanium-rich oxide mineral from the Eastern Bushveld Complex. American Mineralogist, 63, 37–39.

Cameron, K.L., and Cameron, M. (1973) Mineralogy of ultramafic nodules from Knippa Quarry, near Uvalde, Texas. Geological Society of America Abstracts with Programs, 5, 566.

Chase, M.W., Jr., Davies, C.A., Downey, J.R., Jr., Frurip, D.J., McDonald, R.A., and Syverud, A.N. (1985) JANAF thermochemical tables, third edition. Journal of Physical and Chemical Reference Data, 14, Supplement 1, 1856 p.

Doss, B. (1892) Über eine zufällige Bildung von Pseudobrookit, Hämatit und Anhydrit als Sublimationsprodukt, und über die systematische Stellung des ersteren. Zeitschrift für Kristallographie und Mineralogie, 20, 566–587.

El Goresy, A., and Chao, E.C.T. (1976) Identification and significance of armalcolite in the Ries glass. Earth and Planetary Science Letters, 30, 200–208.

El Goresy, A., Ramdohr, P., and Medenbach, O. (1973) The opaque minerals in Apollo 17 samples. Eos, 54, 591–592.

El Goresy, A., Ramdohr, P., Medenbach, O., and Bernhardt, H. (1974) Taurus-Littrow TiO_2-rich basalts: Opaque mineralogy and geochemistry. Proceedings of the 5th Lunar Science Conference, 1, 627–652.

Elkins, L.T., and Grove, T.L. (1990) Ternary feldspar experiments and thermodynamic models. American Mineralogist, 75, 544–559.

Evans, L.G., and Muan, A. (1971) Activity-composition relations and stabilities of end-member compounds in the system MgO-NiO-TiO_2 in contact with metallic nickel at 1400 °C. Thermochimica Acta, 2, 121–134.

Fei, Y., and Saxena, S.K. (1986) A thermochemical data base for phase equilibria in the system Fe-Mg-Si-O at high pressure and temperature. Physics and Chemistry of Minerals, 13, 311–324.

Friel, J.J., Harker, R.I., and Ulmer, G.C. (1977) Armalcolite stability as a function of pressure and oxygen fugacity. Geochimica et Cosmochimica Acta, 41, 403–410.

Frost, B.R. (1991) Introduction to oxygen fugacity and its petrologic importance. In Mineralogical Society of America Reviews in Mineralogy, 25, 1–9.

Fuhrman, M.L., and Lindsley, D.H. (1988) Ternary-feldspar modeling and thermometry. American Mineralogist, 73, 201–215.

Fyfe, W.S., and Verhoogen, J. (1958) General thermodynamic considerations. In Geological Society of America Memoir, 73, 21–51.

Ghiorso, M.S. (1990) Thermodynamic properties of hematite-ilmenite-geikielite solid solutions. Contributions to Mineralogy and Petrology, 104, 645–667.

Grey, I.E., and Ward, J. (1973) An X-ray and Mössbauer study of the $FeTi_2O_5$-Ti_3O_5 system. Journal of Solid State Chemistry, 7, 300–307.

Haggerty, S.E. (1973a) Armalcolite paragenesis and subsolidus reduction of chromian-ülvospinel and chromian-picroilmenite. Eos, 54, 593–594.

——— (1973b) Armalcolite and genetically associated opaque minerals in the lunar samples. Proceedings of the 4th Lunar Conference, 1, 777–797.

——— (1973c) Ortho and para-armalcolite samples in Apollo 17. Nature, 242, 123–125.

——— (1975) The chemistry and genesis of opaque minerals in kimberlites. Physics and Chemistry of the Earth, 9, 295–307.

——— (1978) The Allende meteorite: Solid solution characteristics and

the significance of a new titanate mineral series in association with armalcolite. Proceedings of the 9th Lunar and Planetary Science Conference, 1, 1331–1344.

——— (1983) The mineral chemistry of new titanates from Jagersfontein kimberlite, South Africa: Implications for metasomatism in the upper mantle. Geochimica et Cosmochimica Acta, 47, 1833–1854.

——— (1987) Metasomatic mineral titanates in upper mantle xenoliths. In P.H. Nixon, Ed., Mantle xenoliths, p. 671–690. Wiley, New York.

Haggerty, S.E., and Lindsley, D.H. (1969) Stability of the pseudobrookite (Fe_2TiO_5)-ferropseudobrookite ($FeTi_2O_5$) series. Carnegie Institution of Washington Year Book, 68, 247–249.

Haggerty, S.E., Bell, P.M., Finger, L.W., and Bryan, W.B. (1970) Iron-titanium oxides and olivine from 10020 and 10071. Science, 167, 613–615.

Hartzman, M.J., and Lindsley, D.H. (1973) The armalcolite join ($FeTi_2O_5$-$MgTi_2O_5$) with and without excess Fe^0: Indirect evidence for Ti^{3+} on the moon. Geological Society of America Abstracts with Programs, 5, 653–654.

Hayob, J.L. (1994) Xenoliths from central Mexico: Experimental, mineralogical and petrological evidence for high temperature metamorphism of the lower crust, 276 p. Ph.D. thesis, University of Michigan, Ann Arbor, Michigan.

Hayob, J.L., Essene, E.J., Ruiz, J., Ortega-Gutiérrez, F., and Aranda-Gómez, J.J. (1989) Young high-temperature granulites from the base of the crust in central Mexico. Nature, 342, 265–268.

Hayob, J.L., Essene, E.J., and Ruiz, J. (1990) High-temperature granulites: Reply. Nature, 347, 133–134.

Hazen, R.M., and Finger, L.W. (1981) Bulk moduli and high pressure crystal structures of rutile-type compounds. Journal of Physics and Chemistry of Solids, 42, 143–151.

Ishikawa, Y., and Akimoto, S. (1957) Magnetic properties of the $FeTiO_3$-Fe_2O_3 solid-solution series. Journal of the Physical Society of Japan, 12, 1083–1098.

Kelley, K.K., and King, E.G. (1961) Contributions to the data on theoretical metallurgy: XIV. Entropies of the elements and inorganic compounds. U.S. Bureau of Mines Bulletin, 592, 149 p.

Kesson, S.E., and Lindsley, D.H. (1975) The effects of Al^{3+}, Cr^{3+}, and Ti^{3+} on the stability of armalcolite. Proceedings of the 6th Lunar Science Conference, 1, 911–920.

Knacke, O., Kubaschewski, O., and Hesselmann, K. (1991) Thermochemical properties of inorganic substances I and II (2nd edition), 2412 p. Springer-Verlag, New York.

Koziol, A.M., and Newton, R.C. (1988) Redetermination of the anorthite breakdown reaction and improvement of the plagioclase-garnet-Al_2SiO_5-quartz geobarometer. American Mineralogist, 73, 216–223.

Kushiro, I., and Nakamura, Y. (1970) Petrology of some lunar crystalline rocks. Proceedings of the Apollo 11 Lunar Science Conference. Geochimica et Cosmochimica Acta, Supplement 1, 1, 607–626.

Levy, C., Christophe-Michel-Levy, M., Picot, P., and Caye, R. (1972) A new titanium and zirconium oxide from the Apollo 14 samples. Proceedings of the 3rd Lunar Science Conference. Geochimica et Cosmochimica Acta, Supplement 3, 1, 1115–1120.

Liebermann, R.C. (1976) Elasticity of ilmenites. Physics of Earth and Planetary Interiors, 12, 5–10.

Lind, M.D., and Housley, R.M. (1972) Crystallization studies of lunar igneous rocks: Crystal structures of synthetic armalcolite. Science, 175, 521–523.

Lindsley, D.H., and Nekvasil, H. (1989) A ternary feldspar model for all reasons. Eos, 70, 506.

Lindsley, D.H., Kesson, S.E., Hartzmann, M.J., and Cushman, M.K. (1974) The stability of armalcolite: Experimental studies in the system Mg-Fe-Ti-O. Proceedings of the 5th Lunar Science Conference. Geochimica et Cosmochimica Acta, Supplement 5, 521–534.

Lorand, J.P., and Cottin, J.Y. (1987) Ilménite et pseudobrookite (kennedyite) magnésiennes dans les cumulats ultrabasiques de l'intrusion stratifiée occidentale de Laouni, Hoggar méridional (Algérie). Bulletin de Minéralogie, 110, 373–378.

Lufkin, J.L. (1976) Oxide minerals in miarolitic rhyolite, Black Range, New Mexico. American Mineralogist, 61, 425–430.

Luhr, J.F., Aranda-Gómez, J.J., and Pier, J.G. (1989) Spinel-lherzolite-bearing Quaternary volcanic centers in San Luis Potosí, Mexico: I. Geology, mineralogy, and petrology. Journal of Geophysical Research, 94, 7916–7940.

Mets, O.F., Polezhayeva, L.I., and Bogdanova, A.N. (1985) Armalcolite from microcline-plagioclase pegmatites of the Kola Peninsula. International Geology Review, 27, 1470–1480.

Muranaka, S., Shinjo, T., Bando, Y., and Takada, T. (1971) Mössbauer study of Fe_2TiO_5 and $FeTi_2O_5$. Journal of the Physical Society of Japan, 30, 890.

Navrotsky, A. (1975) Thermodynamics of formation of some compounds with the pseudobrookite structure and of the $FeTi_2O_5$-Ti_3O_5 solid solution series. American Mineralogist, 60, 249–256.

Naylor, B.F., and Cook, O.A. (1946) High-temperature heat contents of the metatitanates of calcium, iron and magnesium. Journal of the American Chemical Society, 68, 1003–1005.

Nickel, E.H. (1992) Nomenclature for mineral solid solutions. American Mineralogist, 77, 660–662.

Nordstrom, D.K., and Munoz, J.L. (1986) Geochemical thermodynamics, p. 285–324. Blackwell Scientific, Palo Alto, California.

Ottemann, J., and Frenzel, G. (1965) Der Chemismus der Pseudobrookit von Vulkaniten. Schweizerische Mineralogische und Petrographische Mitteilungen, 45, 819–836.

Palache, C. (1935) Additional notes on pseudobrookite. American Mineralogist, 20, 660–663.

Papike, J.J. Bence, A.E., and Lindsley, D.H. (1974) Mare basalts from the Taurus-Littrow region of the moon. Proceedings of the 5th Lunar Conference, 1, 471–504.

Peckett, A., Phillips, R., and Brown, G.M. (1972) New zirconium-rich minerals from Apollo 14 and 15 lunar rocks. Nature, 236, 215–217.

Pederson, A.K. (1981) Armalcolite-bearing Fe-Ti oxide assemblages in graphite-equilibrated salic volcanic rocks with native iron from Disko, central west Greenland. Contributions to Mineralogy and Petrology, 77, 307–324.

Powneeby, M.I., Wall, V.J., and O'Neill, H.S.C. (1987) Fe-Mn partitioning between garnet and ilmenite: Experimental calibration and applications. Contributions to Mineralogy and Petrology, 97, 116–126.

Reid, A.M., Warner, J.L., Ridley, W.I., and Brown, R.W. (1973) Luna 20 soil: Abundance and composition of phases in the 45–125 micron fraction. Geochimica et Cosmochimica Acta, 37, 1011–1030.

Rice, J.M., Dickey, J.S., Jr., and Lyons, J.B. (1971) Skeletal crystallization of pseudobrookite. American Mineralogist, 56, 158–162.

Robie, R.A., Hemingway, B.S., and Fisher, J.R. (1978) Thermodynamic properties of minerals and related substances at 298.15 K and 1 bar pressure (10^5 Pascals) and at higher temperatures. U.S. Geological Survey Bulletin, 1452, 456 p.

Robinson, G.R., Jr., Hass, J.L., Jr., Schafer, C.M., and Haselton, H.T., Jr. (1982) Thermodynamic properties of selected phases in the MgO-SiO_2-H_2O-CO_2, CaO-Al_2O_3-SiO_2-H_2O-CO_2, and FeO-Fe_2O_3-SiO_2 chemical systems with special emphasis on the properties of basalts and their mineral components. U.S. Geological Survey Open-File Report 83-79, 429 p.

Ryzhenko, B.N., and Volkov, V.P. (1971) Fugacity coefficients of some gases in a broad range of temperatures and pressures. Geochemistry International, 12, 468–481.

Schaller, W.T. (1912) The rutile group minerals. U.S. Geological Survey Bulletin, 509, 8–39.

Shmulovich, K.I., and Shmonov, V.M. (1975) Fugacity coefficients for CO_2 from 1.0132 to 10,000 bar and 450 to 1300 K. Geochemistry International, 12, 202–206.

Skinner, B.J. (1966) Thermal expansion. In Geological Society of America Memoir, 97, 75–96.

Smith, D.G.W. (1965) The chemistry and mineralogy of some emery-like rocks from Sithean Sluaigh, Strachur, Argyllshire. American Mineralogist, 50, 1982–2022.

Smyth, J.R. (1974) The crystal chemistry of armalcolites from Apollo 17. Earth and Planetary Science Letters, 24, 262–270.

Stanin, F.T., and Taylor, L.A. (1980) Armalcolite: An oxygen fugacity indicator. Proceedings of the 11th Lunar and Planetary Science Conference, 1, 117–124.

Steele, I.M. (1974) Ilmenite and armalcolite in Apollo 17 breccias. American Mineralogist, 59, 681–689.

Stickler, J.J., Kern, S., Wold, A., and Heller, G.S. (1967) Magnetic reso-

nance and susceptibility of several ilmenite powders. Physical Review, 164, 765–767.

Stormer, J.C., and Zhu, J. (1994) Pseudobrookite and Ti-phlogopite from a high temperature vapor phase assemblage in alkali olivine basalt. Eos, 75, 356.

Tiedemann, P., and Müller-Buschbaum, H. (1982) Zum problem der metallverteilung in pseudobrookiten: $FeAlTiO_5$ und Fe_2TiO_5. Zeitschrift für anorganische und allgemeine Chemie, 494, 98–102.

Traube, H. (1892) Ueber den Pseudobrookit vom Aranyer Berge in Siebenbürgen. Zeitschrift für Kristallographie und Mineralogie, 20, 327–331.

Tsymbal, S.N., Tatarintsev, V.I., Legkova, G.V., and Yegorova, L.N. (1980) Armalcolite: The first occurrence in the USSR. Mineralogiya Zhurnal, 2, 87–95 (in Russian).

Tsymbal, S.N., Tatarintsev, V.I., Garanin, V.K., and Kudryatseva, G.P. (1982) Armalcolite and constituent minerals of ores which are associated with trachybasalts of Pripet shock. Mineralogiya Zhurnal, 4, 28–36 (in Russian).

van Kooten, G.K. (1980) Mineralogy, petrology and geochemistry of an ultrapotassic basaltic suite, central Sierra Nevada, California, U.S.A. Journal of Petrology, 21, 651–684.

Varlamov, D.A., Garanin, V.K., and Kostrovitsky, S.J. (1993) Unusual association of ore minerals in inclusion of garnet from international kimberlite pipe. Russian Academy, Doklady Nauk, 328, 596–600.

Velde, D. (1975) Armalcolite-Ti-phlogopite-diopside-analcite-bearing lamproites from Smoky Butte, Garfield County, Montana. American Mineralogist, 60, 566–573.

Virgo, D., and Huggins, F.E. (1975) Cation distributions in some compounds with the pseudobrookite structure. Carnegie Institution of Washington Year Book, 74, 585–590.

Vlassopoulos, D., Rossman, G.R., and Haggerty, S.E. (1993) Coupled substitution of H and minor elements in rutile and the implications of high OH contents in Nb- and Cr-rich rutile from the upper mantle. American Mineralogist, 78, 1181–1191.

von Knorring, O., and Cox, K.G. (1961) Kennedyite, a new mineral of the pseudobrookite series. Mineralogical Magazine, 32, 676–682.

Wechsler, B.A. (1977) Cation distribution and high-temperature crystal chemistry of armalcolite. American Mineralogist, 62, 913–920.

Wechsler, B.A., and Navrotsky, A. (1984) Thermodynamic and structural chemistry of compounds in the system MgO-TiO_2. Journal of Solid State Chemistry, 55, 165–180.

Wechsler, B.A., and Prewitt, C.T. (1984) Crystal structure of ilmenite ($FeTiO_3$) at high temperature and at high pressure. American Mineralogist, 69, 176–185.

Wechsler, B.A., and von Dreele, R.B. (1989) Structure refinements of Mg_2TiO_4, $MgTiO_3$ and $MgTi_2O_5$ by time-of-flight neutron powder diffraction. Acta Crystallographica, B45, 542–549.

Wechsler, B.A., Prewitt, C.T., and Papike, J.J. (1976) Chemistry and structure of lunar and synthetic armalcolite. Earth and Planetary Science Letters, 29, 91–103.

Williams, K.L., and Taylor, L.A. (1974) Optical and chemical properties of Apollo 17 armalcolites. Geology, 2, 5–8.

Manuscript received June 1, 1994
Manuscript accepted March 24, 1995